A vacuolar phosphate transporter essential for phosphate homeostasis in *Arabidopsis*

Jinlong Liu[a], Lei Yang[a], Mingda Luan[a], Yuan Wang[a], Chi Zhang[a], Bin Zhang[a], Jisen Shi[b], Fu-Geng Zhao[a,1], Wenzhi Lan[a,1], and Sheng Luan[a,c,1]

[a]State Key Laboratory for Pharmaceutical Biotechnology, Nanjing University–Nanjing Forestry University Joint Institute for Plant Molecular Biology, College of Life Sciences, Nanjing University, Nanjing 210093, China; [b]Nanjing University–Nanjing Forestry University Joint Institute for Plant Molecular Biology, Key Laboratory of Forest Genetics and Biotechnology, Nanjing Forestry University, Nanjing 210037, China; and [c]Department of Plant and Microbial Biology, University of California, Berkeley, CA 94720

Edited by Natasha V. Raikhel, Center for Plant Cell Biology, Riverside, CA, and approved October 21, 2015 (received for review July 24, 2015)

Inorganic phosphate (Pi) is stored in the vacuole, allowing plants to adapt to variable Pi availability in the soil. The transporters that mediate Pi sequestration into vacuole remain unknown, however. Here we report the functional characterization of Vacuolar Phosphate Transporter 1 (VPT1), an SPX domain protein that transports Pi into the vacuole in *Arabidopsis*. The *vpt1* mutant plants were stunted and consistently retained less Pi than wild type plants, especially when grown in medium containing high levels of Pi. In seedlings, *VPT1* was expressed primarily in younger tissues under normal conditions, but was strongly induced by high-Pi conditions in older tissues, suggesting that VPT1 functions in Pi storage in young tissues and in detoxification of high Pi in older tissues. As a result, disruption of *VPT1* rendered plants hypersensitive to both low-Pi and high-Pi conditions, reducing the adaptability of plants to changing Pi availability. Patch-clamp analysis of isolated vacuoles showed that the Pi influx current was severely reduced in *vpt1* compared with wild type plants. When ectopically expressed in *Nicotiana benthamiana* mesophyll cells, VPT1 mediates vacuolar influx of anions, including Pi, SO_4^{2-}, NO_3^-, Cl^-, and malate with Pi as that preferred anion. The VPT1-mediated Pi current amplitude was dependent on cytosolic phosphate concentration. Single-channel analysis showed that the open probability of VPT1 was increased with the increase in transtonoplast potential. We conclude that VPT1 is a transporter responsible for vacuolar Pi storage and is essential for Pi adaptation in *Arabidopsis*.

vacuolar phosphate sequestration | anion channel | patch clamp | phosphorus nutrition

Phosphorus (P) is a critical component of many metabolites and macromolecules, including ATP, phospholipid, and nucleic acid, and participates in numerous biochemical pathways, including gene expression and signal transduction, among many others. A major source of P element in the biological systems comes from the soil from which plants absorb soluble forms of P-containing molecules and metabolize them into organic forms. As the major form of soluble P, inorganic phosphate (Pi) is present in the soil at low levels and is often a limiting factor for plant growth and productivity. The acquisition and translocation of Pi by plant roots have been the focus of numerous studies identifying transport proteins involved in the uptake and distribution of Pi in plants (1–4).

Although the Pi concentration in soil is usually low, it can be increased by microbial activity and by the application of fertilizers for agricultural crop production (2). Thus, Pi availability in soil often changes, requiring plants to develop mechanisms to adapt to such changes and maintain Pi homeostasis in the cell. When soil Pi levels are high, excess Pi is sequestered in the vacuole to prevent toxicity to the cytoplasm and serve as a Pi store (5). When soil Pi levels are low, the vacuolar Pi pool will supply Pi to the cytoplasm in support of biochemical pathways (6, 7). According to ^{31}P-NMR analyses, Pi concentration is much higher in the vacuole than in the cytosol (7, 8), indicating that the vacuole is the major Pi store. Although a strong mechanism is essential for vacuolar Pi sequestration in higher plants, there is little knowledge regarding molecular identity of transport proteins in the vacuolar membrane (tonoplast).

So far, vacuolar phosphate transporters have been studied mainly in the yeast model, *Saccharomyces cerevisiae*. The yeast vacuolar protein complex responsible for vacuolar polyphosphate accumulation consists of four transmembrane proteins: ScVTC1 (vacuolar transporter chaperone 1), ScVTC2, ScVTC3, and ScVTC4 (9). Another tonoplast Pi transporter, ScPHO91, is mainly responsible for vacuolar Pi efflux to the cytoplasm under low-Pi conditions (10). Interestingly, ScVTC2/3/4 and ScPHO91 share a common feature, the presence of the SPX domain [named after yeast Syg1 and Pho81 and human xenotropic and polytropic retrovirus receptor 1 (XPR1)]. The SPX proteins also exist in plants, and some of them have been shown to play a role in Pi nutrition (11).

In *Arabidopsis*, there are four protein families containing SPX domains, including SPX, SPX-RING, SPX-EXS, and SPX-MFS. The members of the first two families contain no transmembrane domains. The nucleus-localized SPX1 is a negative regulator of Pi starvation responses through inhibiting the activity of PHOSPHATE STARVATION RESPONSE REGULATOR 1 (PHR1) (12). As a member of the SPX-RING family with the RING-type ubiquitin ligase activity, NITROGEN LIMITATION ADAPTATION (AtNLA) may regulate protein degradation of some Pi transporters to maintain Pi homeostasis in a nitrate-dependent manner (13, 14). The SPX-EXS family consists of 11 members that contain multiple transmembrane domains,

Significance

Phosphate is an essential nutrient for plant growth, and inorganic phosphate (Pi) is stored largely in the vacuole of plant cells. Thus, vacuolar Pi maintains homeostasis of cytosolic Pi to ensure an optimal Pi supply for plants under variable Pi status in the soil. This study uncovered in *Arabidopsis* a vacuolar phosphate transporter, VPT1, that mediates vacuolar Pi sequestration. Lack of VPT1 caused growth defects under both low-Pi and high-Pi conditions, implicating VPT1 in plant adaptation to constantly changing Pi levels in the environment. This finding not only supplies a missing link in our understanding of vacuolar Pi storage and homeostasis, but also provides a new path for engineering crops that can better adapt to variable Pi availability in the soil.

Author contributions: J.L., F.-G.Z., W.L., and S.L. designed research; J.L., L.Y., M.L., C.Z., and F.-G.Z. performed research; L.Y., M.L., Y.W., C.Z., B.Z., J.S., and F.-G.Z. contributed new reagents/analytic tools; J.L., L.Y., M.L., F.-G.Z., W.L., and S.L. analyzed data; and J.L., F.-G.Z., W.L., and S.L. wrote the paper.

The authors declare no conflict of interest.

This article is a PNAS Direct Submission.

[1]To whom correspondence may be addressed. Email: fgzhao@nju.edu.cn, lanw@nju.edu.cn, or sluan@berkeley.edu.

This article contains supporting information online at www.pnas.org/lookup/suppl/doi:10.1073/pnas.1514598112/-/DCSupplemental.

characteristic of transporters. Indeed, two members of this family, the Golgi-located PHO1 (PHOSPHATE 1) and PHO1; H1, are shown to function in Pi translocation (15, 16). The SPX-MFS family, like SPX-EXS, also contains a group of proteins containing multitransmembrane domains. There are three members in the *Arabidopsis* SPX-MFS family, but the function of none of them has been characterized to date. Using a combination of genetic and electrophysiological approaches, we show here that one of these, Vacuolar Phosphate Transporter 1 (VPT1), functions as a phosphate transporter essential for vacuolar Pi sequestration, bridging a gap in our understanding of Pi homeostasis in plant cells.

Results

VPT1 Functions in Plant Adaptation to Variable Pi Status in the Environment. In search of vacuolar Pi transporters in plants, we focused our efforts on a functional analysis of the SPX-MFS family members, for several reasons. First, among the four *Arabidopsis* SPX domain-containing protein families (*SI Appendix*, Fig. S1*A*), three of them—SPX, SPX-EXS, SPX-RING—have been functionally connected to Pi nutrition (12–16). We suspected that the function of the fourth family, SPX-MFS, is also linked to Pi nutrition. Second, the three members in the *Arabidopsis* SPX-MFS family are the most closely related to yeast vacuolar phosphate transporters, such as ScVTCs and PHO91 (*SI Appendix*, Fig. S1*A*). These members contain 10~11 transmembrane domains according to TMHMM analysis (www.cbs.dtu.dk/services/TMHMM/), and have a long N-terminal tail and a large loop in the middle. We present a topological model of protein product encoded by *At1g63010.1* as an example (*SI Appendix*, Fig. S1*B*). These structural features are characteristic of a transporter. Third, a proteomic study indicated that *Arabidopsis* SPX-MSF family members are associated with tonoplast fractions in *Arabidopsis* plants (17). Finally, a related protein, OsPSX-MSF1, has been linked to the Pi content in rice leaves (18). Taken together, the foregoing studies suggest that members of the SPX-MFS family are qualified candidates for vacuolar Pi transporters.

We began to test this hypothesis by genetic analysis of these genes using T-DNA insertional mutants of *Arabidopsis*. Among the three genes in the SPX-MFS cluster, we obtained the knockout (KO) mutants of *At1g63010* and *At4g22990*. The KO mutant of *At4g22990* did not show any phenotypic changes compared with the WT plant under variable Pi conditions. Thus, in this report we focus on the characterization of a KO mutant of *At1g63010* (Fig. 1 *A* and *B*), because this mutant was stunted under normal growth conditions in soil (Fig. 1 *C* and *D*) and even more so under high-Pi conditions in hydroponic culture (Fig. 1 *E* and *F*). We named the gene *At1g63010* as *Vacuolar Phosphate Transporter 1* (*VPT1*) based on our research described in this report.

We further confirmed that the phenotype of the *vpt1* mutant resulted from lack of VPT1 function by complementation using a genomic fragment of the *VPT1* gene (Fig. 1 *B–F*). Along with reductions in seedling biomass and root length (Fig. 1 *C–F*), earlier flowering and reduced seed yield were also apparent in the mutant plants grown in soil (*SI Appendix*, Fig. S2). We further analyzed root growth in the hydroponic culture under different Pi concentrations. Only under a very low Pi level (1.3 μM; Fig. 2*A*) did the *vpt1* mutant appear similar to the wild type. As the Pi concentration increased, root elongation in the *vpt1* seedlings was severely inhibited compared with the wild type. Interestingly, the higher the Pi levels in the medium, the more severely inhibited the seedling growth and root elongation (Fig. 2 *A–C*). Stunted growth of *vpt1* was also apparent when grown on 0.5× Murashige and Skoog (MS) agar medium (*SI Appendix*, Fig. S3) or in the nutrient-sufficient soil (*SI Appendix*, Fig. S4). Under both conditions, Pi levels were in the millimolar range (*SI Appendix*, Figs. S3 and S4), consistent with the results obtained under hydroponic conditions (Fig. 2).

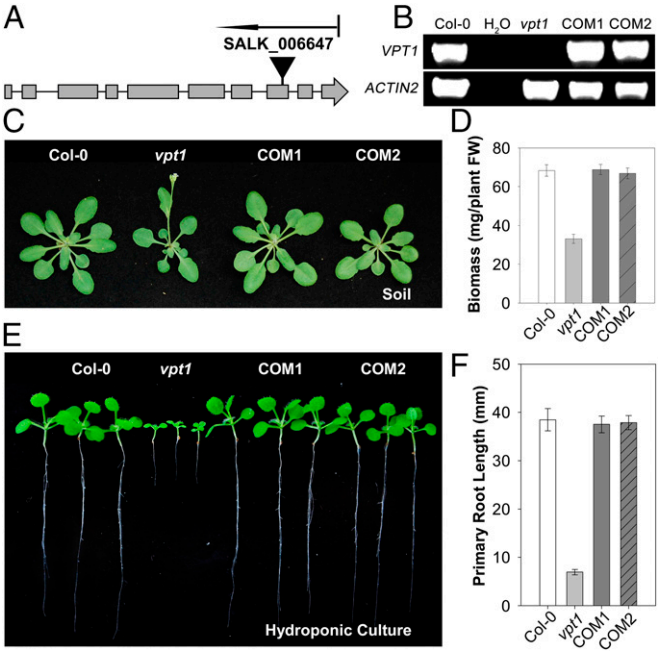

Fig. 1. Genetic characterization and phenotypic analysis of *vpt1* mutant plants. (*A*) Scheme of the *Arabidopsis VPT1* gene structure and localization of the T-DNA insertion site of SALK_006647. Solid boxes and lines indicate exons and introns, respectively. The position of the T-DNA insertions in *vpt1* is indicated by a solid triangle. (*B*) qRT-PCR analysis of *VPT1* and *ACTIN2* mRNA levels in wild type (Col-0), water, *vpt1* mutant plants (*vpt1*), and two complementation lines transformed with *At1g63010* genomic DNA (COM1 and COM2). (*C*) Phenotype of wild type (Col-0), *vpt1*, COM1, and COM2 plants grown in soil for 3 wk. (*D*) Comparative analysis of the aerial biomass in 3-wk-old seedlings of various genotypes as in *C*. Three independent experiments were performed. Values are mean ± SD. $n = 12$ for each genotype. (*E* and *F*) Growth phenotype (*E*) and primary root length (*F*) of 2-wk-old wild type (Col-0), *vpt1*, COM1, and COM2 plants grown in hydroponic culture containing 6.5 mM Pi. Three independent experiments were performed. Data are mean ± SD. $n = 16$ for each genotype. The plants shown in *C* and *E* were planted at a light intensity of 150 μmol/m^2/s with a long-day cycle (16 h light/8 h dark).

Pi overdose in the environment is toxic to plants (5). Under the conditions used in this study, high Pi levels in the medium not only inhibited plant growth, but also caused plant death (*SI Appendix*, Fig. S5). When grown in the medium containing millimolar levels of Pi, the death rate of *vpt1* mutant seedlings was much higher than that of wild type (*SI Appendix*, Fig. S5), further supporting the conclusion that disruption of the *VPT1* gene rendered the plants more sensitive to high Pi toxicity.

In addition to its detoxification action, Pi stored in the vacuole is also an important resource for coping with the Pi deficiency often encountered by plants during their life cycle. If VPT1 functions in vacuolar Pi sequestration, then its mutant would have a smaller Pi pool under Pi-sufficient conditions, and, logically, less Pi would be available when transferred to Pi-deficient conditions. Indeed, *vpt1* mutant plants suffered more than wild type plants after the change from a Pi-sufficient to a Pi-deficient condition (Fig. 2*D*). Pi deficiency leads to accumulation of anthocyanin in leaves (19), which was more severe in the *vpt1* mutant than in the wild type (Fig. 2*E*). Consistent with this observation, Pi starvation response genes were induced to a higher level in the mutant *vpt1* compared with the wild type after the plants were transferred to the low-Pi condition. In contrast, the same gene markers were expressed at a lower level in the mutant when the plants remained in Pi-sufficient condition, indicating that cytosolic Pi levels were higher in the mutant owing to a defect in vacuolar sequestration (*SI Appendix*, Fig. S6).

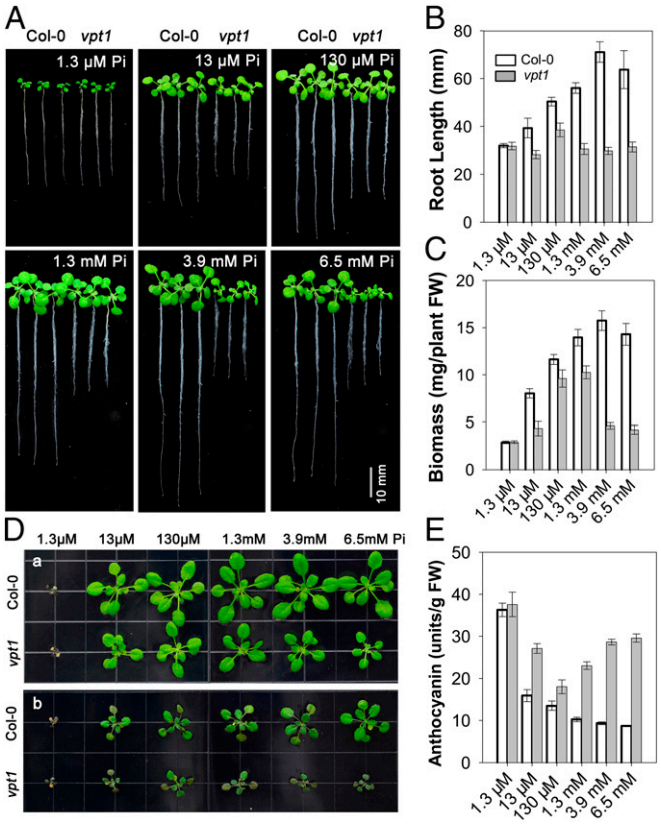

Fig. 2. Growth phenotype of *vpt1* mutants under variable Pi conditions. (*A*) Growth phenotype of 2-wk-old wild type (Col-0) and *vpt1* mutants in hydroponic medium containing 1.3 μM, 13 μM, 130 μM, 1.3 mM, 3.9 mM, or 6.5 mM Pi. (*B* and *C*) Quantitative analyses of primary root length (*B*) and whole-plant biomass (*C*) of wild type (Col-0) and *vpt1* seedlings under the various Pi concentrations as described in *A*. Sixteen 2-wk-old seedlings of wild type (Col-0) and *vpt1* mutants were gathered for root length measurements with Image J software and biomass analysis. Three independent experiments were performed. Data are mean ± SD. (*D*) The phenotype of wild type (Col-0) and *vpt1* plants transplanted from various Pi concentrations to the Pi-deficient condition. The wild type (Col-0) and *vpt1* mutants were grown in hydroponic medium containing 1.3 μM, 13 μM, 130 μM, 1.3 mM, 3.9 mM, or 6.5 mM Pi for 14 d (*a*), and then transferred to medium containing 1.3 μM Pi and grown for another 7 d (*b*). (*E*) Anthocyanin content in the leaves of plants described in *D*. Four independent experiments were performed. Data are mean ± SD.

VPT1 Is Required for Pi Accumulation in Plants. Plants absorb Pi through plasma membrane transporters and accumulate the large majority of Pi in the vacuole (2, 8). Especially under high-Pi conditions, plants often take up more Pi and store excessive Pi in the vacuole (20). If the vacuole sequestration mechanism is defective, then plants would become more sensitive to high-Pi toxicity and at the same time accumulate less Pi.

We noted above that a lack of VPT1 led to high Pi toxicity in the mutant plants. To test whether the *vpt1* mutant is defective in Pi retention, we measured the Pi content in both wild type and mutant seedlings. In all cases, the *vpt1* mutant plants consistently retained less Pi compared with the wild type, regardless of Pi concentrations in the culture medium (Fig. 3*A*). With the increased Pi concentration in the growth medium, the Pi content in wild type plants steadily increased, but the Pi content in *vpt1* mutant plants quickly plateaued at a rather low level (Fig. 3 *A* and *B*). Because the *vpt1* plants were smaller in stature, we suspected that this size difference could possibly affect the comparability of Pi measurements in the wild type and mutant plants. Thus, we constructed a dexamethasone (DEX)-inducible *VPT1* expression system (InVPT1) in the *vpt1* mutant background. Spraying with 10 μM DEX induced *VPT1* expression and promoted Pi accumulation in parallel (*SI Appendix*, Fig. S7). This result again links *VPT1* with Pi retention in *Arabidopsis*, and supports the hypothesis that VPT1 functions in vacuolar Pi sequestration.

The expression pattern of the *VPT1* gene in *Arabidopsis* plants also supports its possible function as a vacuolar Pi storage transporter. According to the results of histochemical β-glucuronidase (GUS) staining of transgenic plants expressing a *VPT1* promoter–*GUS* fusion (Fig. 3*C*), the *VPT1* promoter was more active in the younger tissues in both leaves and roots during vegetative growth. In the 3-wk-old seedlings, the *VPT1*expression level in the young leaves was 3.5-fold greater than that in the older leaves (Fig. 3*D*). With the increasing Pi concentration in the growth medium, the expression of *VPT1* was strongly induced in both roots and leaves (Fig. 3*E*). Interestingly, a detailed analysis of *VPT1* expression in leaves of different ages indicated that Pi induction occurred more strongly in old leaves than in young leaves (Fig. 3*F*), supporting the role of old leaves as "detoxifying organs" for the protection of the young leaves. Indeed, under normal conditions, the Pi content was higher in the younger leaves (Fig. 3*G*), which correlated well with the *VPT1* expression levels in leaves of different ages (Fig. 3*D*). Under high-Pi conditions, the increasing Pi accumulation occurred mainly in the older leaves (Fig. 3*H*), again consistent with Pi-induced expression of *VPT1* in these leaves (Fig. 3*F*). Not surprisingly, *vpt1* mutant plants did not accumulate more Pi under high Pi conditions, because they lacked the VPT1 function responsible for such accumulation (Fig. 3*H*).

VPT1 Is a Tonoplast Phosphate Transporter for Vacuolar Pi Uptake. Genetic analysis of the *vpt1* mutant suggested that VPT1 functions in vacuolar sequestration. To further support this hypothesis, we conducted experiments to show that VPT1 protein is indeed located in the vacuolar membrane. We also measured the activity of VPT1 in plant vacuoles using a patch-clamp procedure.

To determine the subcellular localization of VPT1, we constructed transgenic plants expressing VPT1-GFP fusion protein (35S:VPT1-GFP^{vpt1}) in the *vpt1* mutant background. If the fusion protein complemented the mutant phenotype, this would indicate that this fusion protein is functional and localized to the correct subcellular compartment. The transgenic plants, like the wild type, grew well in the Pi-rich medium and adapted well to the low-Pi condition after transfer from the Pi-sufficient condition, eliminating the growth defects in the *vpt1* mutant (*SI Appendix*, Fig. S8*A*). Moreover, the Pi content in the leaves of the transgenic plants was restored to the wild type level or even higher (*SI Appendix*, Fig. S8*B*), matching the expression levels of the *VPT1-GFP* mRNA (*SI Appendix*, Fig. S8*C*), indicating that the fusion protein was functional. Examination of the leaf epidermal cells by confocal microscopy revealed that VPT1-GFP was localized to the vacuolar membrane.

As shown in Fig. 4*A*, the VPT1-GFP signal was clearly separated from the plasma membrane stained with red fluorescent probe FM4-64 in the 3-d-old seedlings. On the other hand, the VPT1-GFP signal essentially overlapped with the γ-TIP-mCherry fusion protein (Fig. 4*B*), a tonoplast marker (21). Furthermore, when vacuoles were released from isolated mesophyll protoplasts of the transgenic plant, they showed clear a GFP signal at the tonoplast (Fig. 4C). Thus, we concluded that VPT1 was located in the tonoplast, consistent with an earlier finding from proteomic analysis (17), and this observation provided a prerequisite for our patch-clamp analysis of VPT1 activity in plant vacuoles.

To analyze the activity of VPT1 in Pi transport, we established a patch-clamp procedure to determine the inward currents carried by Pi in vacuoles isolated from *Arabidopsis* mesophyll cells (Fig. 5). As documented previously, "inward" currents are

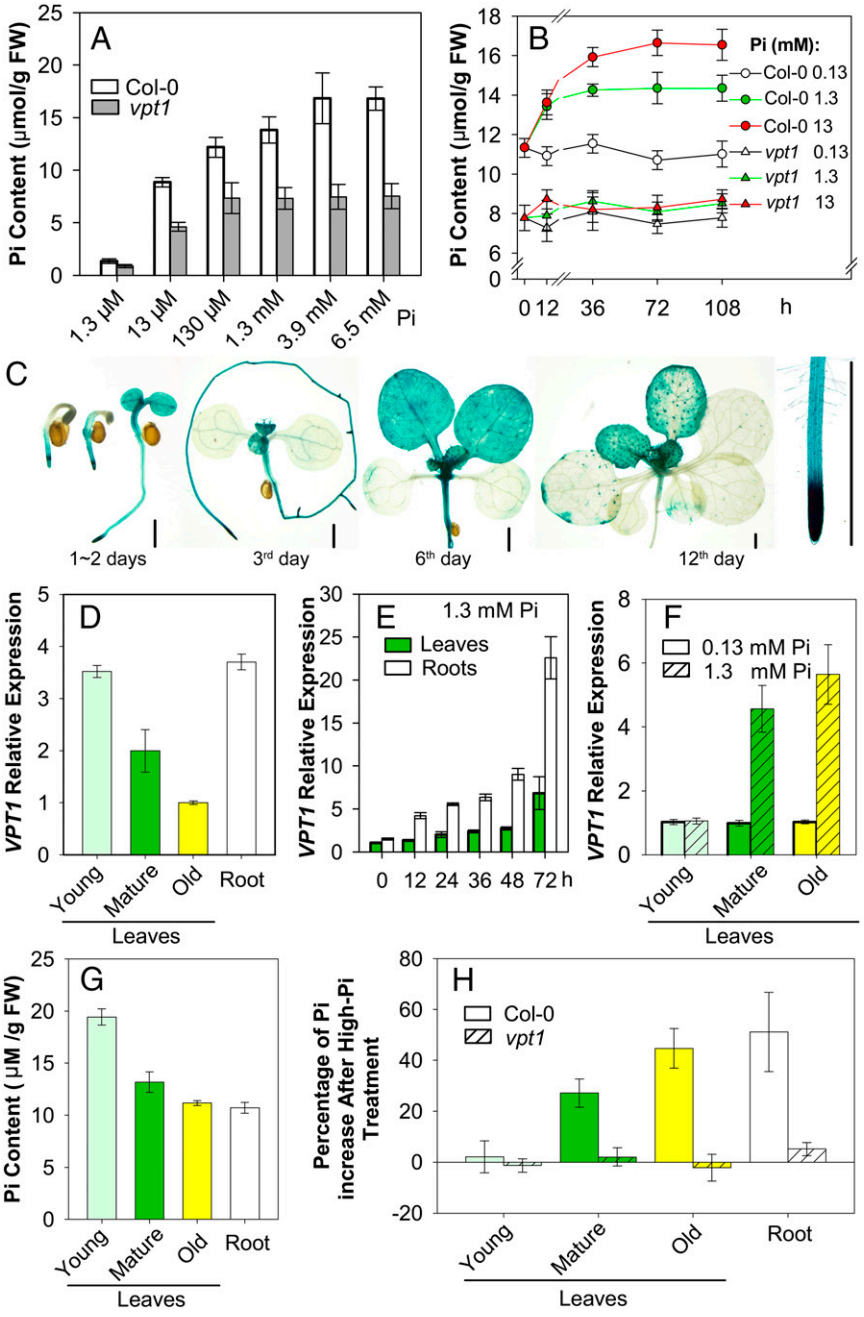

Fig. 3. VPT1 contributes to Pi homeostasis in *Arabidopsis* plants. (*A*) Two-week-old seedlings of *vpt1* mutants contain less Pi than wild type (Col-0) when grown in hydroponic medium with various Pi concentrations. Data are mean ± SD. $n = 5$. (*B*) Time course and dose course of Pi accumulation in the wild type and *vpt1* mutant. Here 3-wk-old wild type (Col-0) and *vpt1* mutants were transferred into the medium containing 0.13 mM, 1.3 mM, or 13 mM Pi, and rosette leaves were collected at the indicated time points for Pi content measurement. Data are mean ± SD. $n = 4$. (*C*) Expression pattern of *pVPT1*::*GUS* in transformed *Arabidopsis* plants. (Scale bar: 2 mm.) (*D*) *VPT1* expression levels in leaves of different ages (young leaves: the upper two leaves that newly emerged; mature leaves: the middle leaves; old leaves: the two true leaves close to the base of plants) and roots of 3-wk-old wild type seedlings grown in the hydroponic solution containing 0.13 mM Pi. Data are mean ± SD. $n = 4$. (*E*) *VPT1* expression levels in leaves and roots of the wild type (Col-0) seedlings after treatment with 1.3 mM Pi. Three-week-old wild type plants (Col-0) cultured in the hydroponic solution containing 0.13 mM Pi were transplanted into the solution containing 1.3 mM Pi, after which rosette leaves and roots were obtained at the indicated time points for mRNA measurement. Data are mean ± SD. $n = 4$. (*F*) *VPT1* expression levels in leaves of different ages from wild type (Col-0) seedlings after treatment with 1.3 mM Pi for 72 h. Data are mean ± SD. $n = 4$. Values were normalized to *ACTIN2*, and the relative expression of *VPT1* was calculated as the ratio of *VPT1* mRNA level to the lowest level (as 1.0) in the group *D*–*F*. (*G*) Pi distribution in the wild-type plants, showing Pi content in roots and leaves of different ages under normal Pi conditions (0.13 mM). (*H*) Percentage of Pi increase in the wild type and *vpt1* mutant plants after high-Pi treatment. Three-week-old seedlings of wild type (Col-0) and mutant *vpt1* plants grown in hydroponic solution containing 0.13 mM Pi were transferred into the solution containing 0.13 mM or 1.3 mM Pi and grown for another 5 d. Leaves of different ages without petioles and roots were collected, and Pi content was measured. Data are mean ± SD. $n = 6$.

defined as movement of a positive charge out of or a negative charge into the vacuole (22). We isolated intact vacuoles from mesophyll cells of wild type and *vpt1* mutant plants and clamped them between +20 and −160 mV with a 0.6-s duration and 20-mV decrements (Fig. 5). Large time-dependent Pi inward currents were recorded in the wild type vacuoles at negative test voltages,

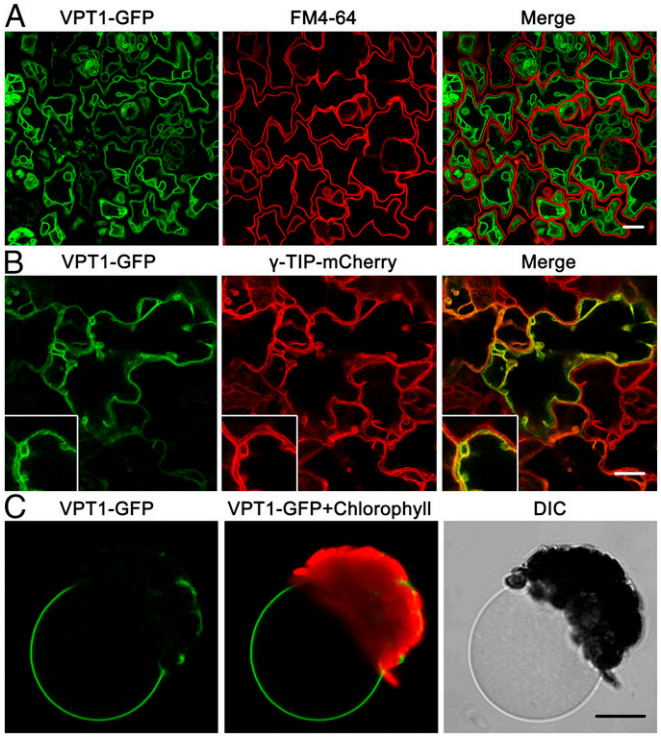

Fig. 4. Subcellular localization of VPT1-GFP in the vacuole membrane. (*A*) Confocal microscopy of GFP signals in the epidermal cells from a cotyledon of a 3-d-old transgenic *vpt1* seedling expressing *35S:VPT1-GFP*. The panels, from left to right, show the GFP signals (green), the plasma membrane fluorescence stained with FM4-64 (red), and an overlay (of green and red) from the same sample. (Scale bar: 10 μm.) (*B*) VPT1-GFP signal overlaid with a γ-TIP-mCherry signal in the epidermal cells from a cotyledon of a 5-d-old seedling expressing *35S:VPT1-GFP* and *35S:γ-TIP-mCherry*. The panels, from left to right, show the GFP signals (green), the mCherry signals (red), and an overlay (of green and red) from the same sample. TIP (a tonoplast intrinsic protein) is a tonoplast marker (21). (*Inset*) The intermembrane space and sag area pressed by nuclei or plastids (21). (*C*) A vacuole released from a mesophyll protoplast isolated from transgenic plants expressing VPT1-GFP. (Scale bar: 10 μm.)

and under the same experimental conditions, the Pi inward currents recorded from *vpt1* mutant vacuoles were much smaller (Fig. 5*A*). At −160 mV, the current density in the mutant vacuole was reduced by >60% compared with the wild type vacuole (Fig. 5*B*). As shown earlier, expression of VPT1-GFP fusion protein in the *vpt1* mutant background complemented the mutant phenotype (*SI Appendix*, Fig. S8). When vacuoles from these plants were isolated and recorded, the Pi current density was also back to the wild type or slightly higher than the wild type (Fig. 5*B*), matching the expression levels of *VPT1-GFP* in the transgenic plants (*SI Appendix*, Fig. S8*C*). These results suggest that VPT1 contributes strongly to the vacuolar Pi influx from the cytosolic side into the vacuolar lumen.

To further confirm that VPT1 mediates Pi influx into the vacuole, we transiently expressed VPT1-GFP in *Nicotiana benthamiana* mesophyll cells and measured the vacuolar Pi current using vacuoles decorated with the GFP signal. In parallel, we used cells transformed with the empty vector alone as a control. As expected, the control vacuoles showed detectable Pi inward currents, similar to those recorded with wild type vacuoles from *Arabidopsis* (Figs. 5*A* and 6*A*); however, in the VPT1-GFP–expressing vacuoles, a much larger Pi inward current was recorded compared with that in the control vacuoles (Fig. 6*A*). On average, the Pi inward current densities in the corresponding vacuoles were increased fivefold by VPT1-GFP overexpression (Fig. 6*B*). Taken together, these results indicate that VPT1 is responsible for a major portion of the Pi inward current in vacuoles under our experimental conditions.

Using the transient expression system, we characterized the VPT1-mediated Pi currents and found that these currents were dependent on cytosolic Pi concentration (Fig. 6 *C*–*E*). When a low level of cytosolic phosphate (1 mM) was applied (100-fold lower than that in the vacuolar lumen), inward current was detectable, albeit at a small amplitude (Fig. 6*C*). When the cytosolic Pi reached a level symmetrical to that in the vacuolar lumen (100 mM Pi_{cyt}/100 mM Pi_{vac}), the current amplitude of the VPT1-GFP vacuole was increased by eightfold (Fig. 6 *C* and *D*). The reversal potentials (E_{rev}) of VPT1 currents shifted to more positive values with increasing cytosolic Pi concentrations (Fig. 6*E*). Furthermore, the E_{rev} values correlated well with the Nernst prediction of phosphate equilibrium potential (Fig. 6*E*), further supporting the idea that the recorded influx current was carried by Pi.

Anion selectivity (Fig. 6*F*) indicated that VPT1 also contributed to the transport of other anions across the tonoplast, but that phosphate transport was increased to the greatest degree by overexpression of VPT1-GFP. Consistent with this transport activity, disruption of *VPT1* expression in the *vpt1* mutant impaired the accumulation of Pi but not of other anions, including sulfate, nitrate, malate, or chloride (*SI Appendix*, Fig. S9). These results further support the notion that the major function of VPT1 is phosphate transport into the vacuole, although VPT1-mediated transport is not strictly selective for Pi.

We further analyzed the single-channel currents in membrane patches detached from vacuoles isolated from *N. benthamiana* mesophyll cells transformed with either empty vector (control) or the *35S:VPT1-GFP* construct. Single-channel activity was not detectable in the control vacuoles. In contrast, we detected single-channel activity in the membrane patches detached from vacuoles isolated from VPT1-GFP–expressing cells. The channel open probability (*Po*) of VPT1 increased with the more negative membrane potentials (Fig. 6*G*). As the membrane potential shifted from −40 mV to −100 mV, the *Po* increased more than 10-fold (Fig. 6*G*). The current amplitude also increased linearly with more negative tonoplast potentials, with a conductance of 59 pS (Fig. 6*H*). The reversal potential of the single channels was

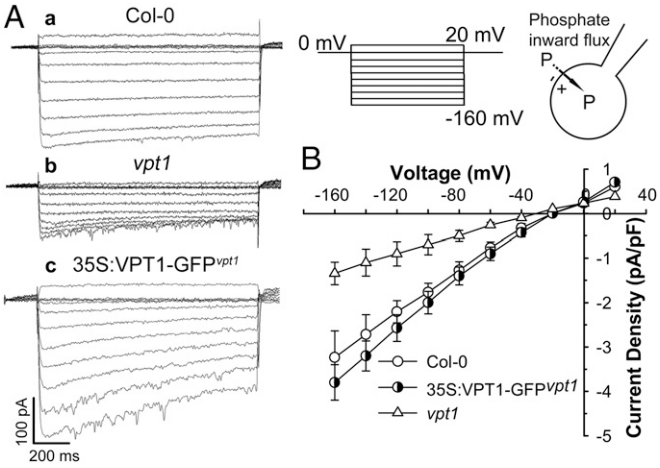

Fig. 5. VPT1 contributes to the Pi current amplitudes recorded in isolated *Arabidopsis* vacuoles. (*A*) The representative current traces were generated by the vacuoles isolated from the wild type (Col-0) (*a*), *vpt1* mutant (*b*), or *35S:VPT1-GFP*^{vpt1} (*c*) leaves. (*B*) The current–voltage relationships were deduced from isolated vacuoles under each condition as in *A*. Data are mean ± SD. $n = 16$. A series of test voltages from 20 to −160 mV in steps of −20 mV with a prepulse holding potential of 0 mV was applied to record currents in the whole-vacuole mode with a symmetrical phosphate condition (100 mM phosphate in cytoplasm/100 mM phosphate in vacuole lumen).

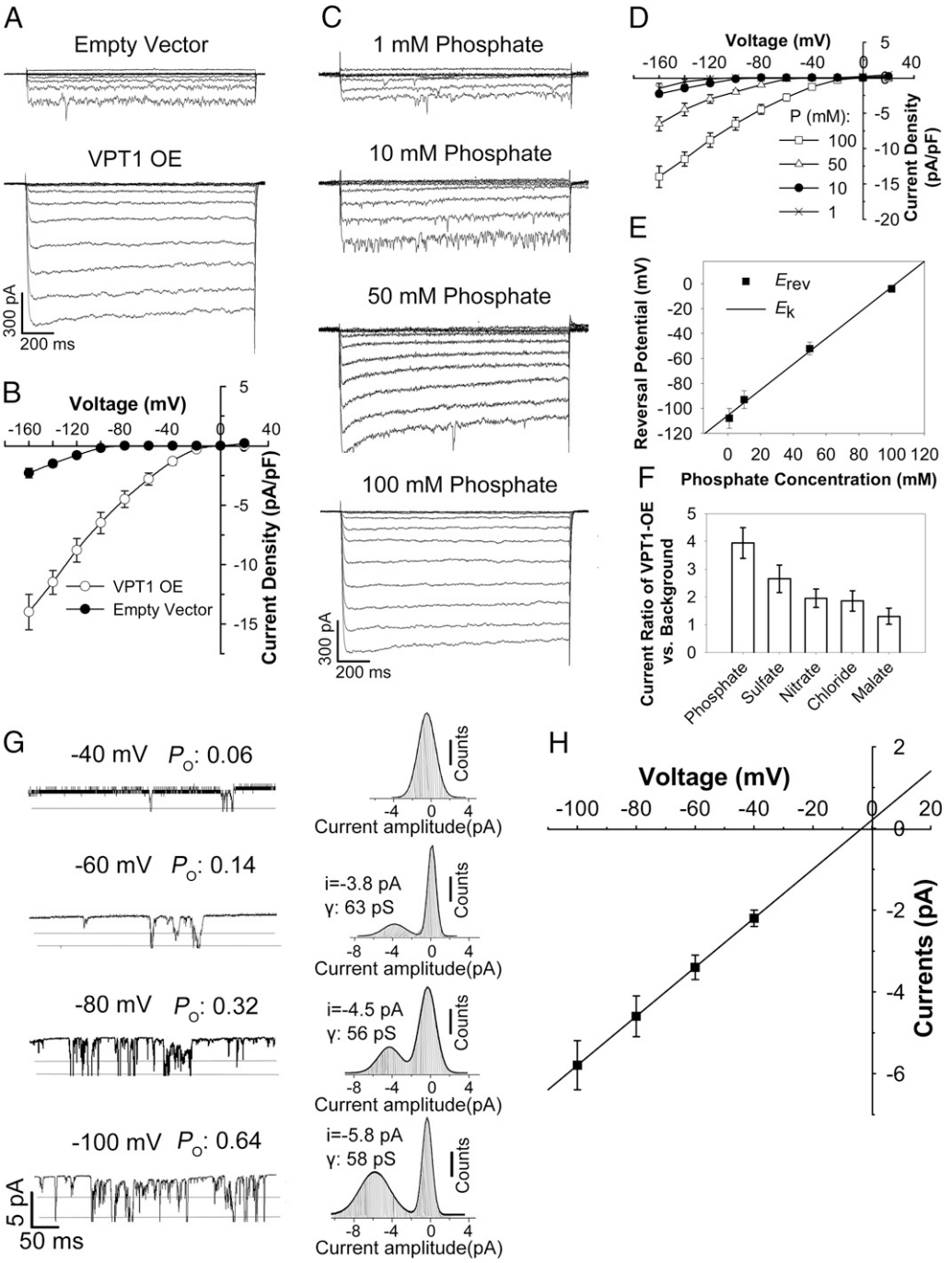

Fig. 6. The *VPT1*-mediated currents in *N. benthamiana* vacuoles are sensitive to phosphate and membrane potentials. (*A* and *B*) *VPT1* expression enhances the currents generated from *N. benthamiana* vacuoles. Shown are typical whole-vacuole current traces (*A*) and the voltage–current relationship (*B*) of channel activities recorded from the mesophyll vacuoles isolated from empty vector-transformed and VPT1-GFP–overexpressing *N. benthamiana* leaves. The isolated vacuoles were bathed in a solution containing 100 mM phosphate. The pipette solution contained 100 mM phosphate. The data in *B* are mean ± SD. $n = 17$. (*C*–*E*) The whole-vacuole currents generated by VPT1-GFP–overexpressing vacuoles were sensitive to the phosphate concentration in bath solution. (*C*) The typical whole-vacuole current traces generated by a VPT1-GFP–expressing vacuole bathed in solution containing 1 mM, 10 mM, 50 mM, or 100 mM phosphate. (*D*) The current–voltage relationship was deduced from recordings of VPT1-GFP–expressing vacuoles as in *C*. The data are mean ± SD. $n = 17$. (*E*) Reversal potentials of phosphate currents at various cytosolic phosphate concentrations. Data points are mean ± SD. The solid line represents the calculated phosphate equilibrium potentials. (*F*) Anion selectivity reflected by the current ratio of VPT1 overexpression (OE) vs. empty vector control. The channel currents at −160 mV were recorded from VPT1-GFP–expressing vacuoles or empty vector-transformed vacuoles bathed in solution containing 100 mM phosphate, sulfate, nitrate, chloride, or malate. The current ratio of VPT1-GFP–tagged vacuoles vs. empty vector-transformed ones was calculated. Data are mean ± SD. $n = 15$. (*G*) The open probability (P_o) of channels in excised outside-out tonoplast patches at different voltages. Representative current traces (*Left*) and corresponding amplitude histograms (*Right*) in an excised outside-out patch recorded at membrane potentials of −40, −60, −80, or −100 mV. (*Left*) The horizontal lines represent the channel open state. (*Right*) The conductance (γ) was calculated as the current-to-voltage ratio. (*H*) Current–voltage relationship of recordings from eight excised outside-out patches under various membrane potentials. Data are mean ± SD.

−3.5 mV, which is very close to the Nernst potential for phosphate [cytosolic (phosphate) = 100 mM; E_{rev} (Pi) = −4 ± 2 mV] (Fig. 6 *E* and *H*).

Discussion

Plant growth requires a large amount of Pi, but Pi levels in most soils are limited and constantly changing. To survive such Pi nutrient "stress" in nature, plants have evolved not only a strong capability of Pi uptake and translocation, but also sophisticated mechanisms to store surplus Pi in the vacuoles to cope with the changing status of soil Pi (2, 20). In fact, the large majority (>90%) of free Pi is stored in the vacuole of a typical expanded plant cell (7, 8). Impaired vacuole storage will directly impact the capacity for Pi accumulation in plants.

Pi acquisition and translocation have been studied extensively over the past two decades (2, 23). Several transporter families have been shown to function in Pi uptake and distribution in plants. These include the phosphate transporters (PHTs) and PHO-type Pi transporters. The plasma membrane-located PHT1s are responsible for the absorption of phosphate, as has been studied in *Arabidopsis* and rice (3, 4, 24, 25). For Pi translocation, the Golgi located PHO1 plays an important role (1, 16). Transport of Pi between the cytosol and chloroplasts involves PHT2;1 and the members of PHT4 family in *Arabidopsis* (26–28). Despite the importance of vacuolar Pi accumulation in plant Pi nutrition, very little is known about the transporters responsible for Pi translocation into the vacuole to achieve Pi homeostasis in the cell. Our study has identified a tonoplast Pi transporter (VPT1) as an essential component in Pi accumulation and plant adaptation to changing Pi status in the environment.

The wild type *Arabidopsis* plants thrived as levels of Pi increased in the culture medium (up to a low millimolar range). As more Pi became available in the medium, plants accumulated more Pi in their cells, as expected, consistent with the idea that surplus Pi may have been stored in the vacuole to avoid toxicity. In contrast, the loss-of- function mutant of VPT1 was dramatically stunted when Pi reached low millimolar levels in the medium. Furthermore, the Pi content in the mutant plants was much lower than that in the wild type plants and failed to increase as Pi concentration rose in the medium. This suggests that VPT1 plays a key role in the accumulation of Pi in plants.

Although lower levels of Pi in the mutant can also result from decrease in uptake, in the context of a Pi-hypersensitive phenotype, it becomes clear that VPT1 functions in vacuolar Pi sequestration. Also consistent with this interpretation is the finding that the *vpt1* mutant suffered more when plants were transferred from high to low Pi conditions. Typically, plants accumulate and store surplus Pi in the vacuole under high-Pi conditions and remobilize the vacuolar Pi to support cell growth under low-Pi conditions. Lack of VPT1 impairs the ability of plants to accumulate Pi in the vacuoles under high-Pi conditions and thus compromises their ability to cope with low Pi.

The results of our genetic analysis strongly implicate VPT1 in vacuolar Pi sequestration. Thus, we decided to directly measure Pi influx using a patch-clamp approach. Although vacuolar Pi efflux current was measured by Dunlop and Phung (29), Pi influx across the vacuolar membrane and the molecular basis of vacuolar Pi transport have not been described. In our study, we first confirmed that VPT1 was indeed localized to the tonoplast, and then used patch-clamping to measure the Pi transport activity mediated by VPT1. In the subcellular localization experiment, we used genetic complementation to ensure functionality of the VPT1-GFP fusion protein before examining its localization, because a protein is functional only after it is correctly targeted in the cell. Indeed, the GFP-VPT1 fusion protein was localized to the tonoplast, because the GFP signal was specifically associated with the tonoplast marker and isolated vacuoles. Analysis of vacuoles from the wild type and *vpt1* mutant plants by the patch-clamp procedure showed that *vpt1* vacuoles displayed a reduced inward current, reflecting impaired Pi influx into the vacuole.

In addition, we also expressed VPT1-GFP fusion in a different plant cell model and confirmed that VPT1 mediates Pi transport into the vacuole. The apparent voltage-gating features and the large conductance revealed by single-channel analysis suggest that VPT1 likely functions as an anion channel (Fig. 6 *G* and *H*). Among the three classes of transporter proteins (pumps, carriers, and ion channels), only ion channels can be measured in an excised patch of membrane (30). The VPT1 single-channel characteristics are comparable to those of vacuolar anion channels described previously (31, 32), and, notably, the VPT1 also has a flickering behavior and a large conductance (Fig. 6 *G* and *H*).

Because the vacuolar membrane potential is favorable for anions flowing into the vacuolar lumen, it is likely that VPT1 functions as an anion channel that prefers Pi over other anions tested in this study. Further work is needed to characterize the detailed biophysical properties of VPT1. Another important area for future work is the identity of transporters responsible for Pi remobilization from vacuole back to the cytosol. The transporters mediating the flux of Pi into and out of vacuole will be important targets for improving crop production under changing Pi conditions.

Materials and Methods

Plant Materials and Growth Conditions. *Arabidopsis thaliana* wild type (ecotype Columbia-0, Col-0) and the T-DNA insertion mutant line (SALK_006647, locus At1g63010) were obtained from the *Arabidopsis* Biological Resource Center. Homozygous individuals were screened by PCR using the primers listed in *SI Appendix*, Table S1. For soil culture, healthy 3-d-old seedlings germinated on 0.5× MS medium [1% (wt/vol) agar, 1% (wt/vol) sucrose] were transferred to the nutrient-rich soil (Pindstrup Mosebrug). For hydroponic culture, we followed a procedure described by Tocquin et al. (33) with different concentrations of NaH_2PO_4 replacing $NH_4H_2PO_4$ as the Pi source. Plants were grown under long-day conditions (16-h illumination of 150 μmol/m^2/s, and 8-h dark cycle) at 22 °C.

Plasmid Constructions and Plant Transformation. For genetic complementation, the full-length genomic DNA of the *VPT1* fragment was amplified from wild type genomic DNA and cloned into the binary vector pCAMBIA-1300. To generate the *VPT1* promoter–GUS construct, the 2,955-bp promoter region upstream of starting codon was amplified and cloned into the pBI-101.1 binary vector, driving the GUS reporter gene. For subcellular localization, the 35S promotor, *VPT1* coding sequence without a stop codon, and *GFP* (*35S:VPT1-GFP*) were cloned into the pCAMBIA-1300. The tonoplast marker, *35S:γ-TIP-mCherry*, was cloned into the pCAMBIA-3301 binary vector. The primers used for plasmids constructions are listed in *SI Appendix*, Table S1. The *Agrobacterium tumefaciens* cells carrying various constructs (GV3101) were used to transform *Arabidopsis* ecotype Col-0, *vpt1* mutant, or *N. benthamiana* plants.

Histochemical Localization of GUS Expression. The GUS staining was done as described by Tian et al. (34), with some modifications. In brief, T3 transgenic seedlings were fixed by incubation in ice-cold 90% (vol/vol) acetone for 15 min and then washed three times with the rinse buffer (50 mM $NaPO_4$ pH 7.2, 1 mM $K_3Fe[CN]_6$, and 1 mM $K_4Fe[CN]_6$). The GUS activity in plant tissues was visualized by incubation in the staining buffer (50 mM $NaPO_4$ pH 7.2, 10 mM Na_2EDTA, 0.1% Triton X-100, 1 mM $K_3Fe[CN]_6$, and 1 mM $K_4Fe[CN]_6$) containing 2 mM 5-bromo-4-chloro-3-indolyl-β-D-glucuronide as a GUS substrate for 6 h in the dark at 37 °C. Individual representative seedlings were photographed after being sufficiently decolorized with 70% (vol/vol) ethanol.

Confocal Microscopy Analyses. The transgenic plants expressing VPT1-GFP (35S: VPT1-GFP^{vpt1}) were grown on 0.5× MS medium for 3–5 d, and the fluorescence signals were examined using an LSM 710 confocal microscope (Zeiss) equipped with an argon/krypton laser. The plasma membrane was stained with 0.1 mg/mL FM4-64 for 5 min, and then washed twice with double-distilled H_2O before microscopic observation. The excitation wavelengths for the GFP, FM4-64, and mCherry signals were 488, 543, and 587 nm, respectively.

Quantitative Real-Time PCR Analysis. Total RNA was extracted from the plantlets grown in the hydroponic system using TRIzol reagent (Invitrogen). The first-strand cDNA was synthesized by M-MLV Reverse Transcriptase (Promega)

with oligo(dT) primers. Quantitative real-time PCR (qRT-PCR) was performed using the QuantiFast SYBR Green PCR Kit (Qiagen) on a CFX Connect Real-Time System (Bio-Rad). Target quantifications were performed with specific primer pairs designed using Primer 5 software (*SI Appendix*, Table S1).

Pi Measurements and Anthocyanin Content Assays. *Arabidopsis* seedlings were grown in the hydroponic system containing different Pi concentrations. Here 50 mg of plant materials and 20 mg of plant leaves were collected for Pi content determination with the ascorbate-molybdate-antimony method as described previously (35) and for anthocyanin determination using the method described by Teng et al. (36), respectively. One anthocyanin unit equals one absorbance unit (A_{530}–$0.25A_{657}$) in 1 mL of extraction solution.

Patch-Clamp Recordings on Isolated Vacuoles. For transient overexpression of VPT1-GFP in *N. bethamiana*, plant growth conditions and agrobacterium-mediated infiltration were as described previously (37). The mesophyll vacuoles of *Arabidopsis* and transformed *N. bethamiana* plants were isolated via a procedure described by De Angeli et al. (31). The ionic currents across the tonoplast were recorded using a standard patch-clamp procedure essentially as described by Beyhl et al. (38). In brief, recordings were performed with the Axon Multiclamp 700B Amplifier (Molecular Devices). The pipette resistance was 5–6 MΩ in the whole-vacuole recording mode and 9–10 MΩ in the single-channel recordings. The pipette solution contained 100 mM H_3PO_4, 1 mM $CaCl_2$, 2 mM $MgCl_2$, and 5 mM Mes-BTP (pH 5.8). The bath solution contained 100 mM H_3PO_4, 6.7 mM EGTA, 5.864 mM $CaCl_2$ (free Ca^{2+} is 2 μM), and 5 mM Mes-BTP (pH 7.0). The osmolality of the pipette and bath solution was adjusted to 550 and 500 mOsm, respectively, with D-sorbitol.

For anion selectivity studies, phosphate in the standard pipette and bath solution was replaced by equimolar amounts of sulfate, nitrate, chloride, or malate. In cytosolic Pi dose-dependent studies, isolated vacuoles were bathed in the bath solution containing various phosphate concentrations as indicated in the figure legends. In the whole-vacuole mode, recording was started at least 10 min after pipette break-in, to equilibrate the vacuolar lumen with the pipette solution.

According to the convention for electrical measurements across endomembranes reported by Bertl et al. (39), the negative currents were corresponded to anions moving from the cytosolic side to the vacuolar lumen. Current recordings were filtered at 2.9 kHz for whole-vacuole recordings and at 1.5 kHz for single-channel recordings. Steady-state currents were calculated by averaging the values during the last 100 ms of each current trace. Considering the variations in the vacuole surface area, the current–voltage relationships were expressed as current density (pA/pF).

ACKNOWLEDGMENTS. We thank the *Arabidopsis* Biological Resource Center for providing *Arabidopsis thaliana* seed stocks and Jiangsu Collaborative Innovation Center for Modern Crop Production for technical support. This work was supported by National Science Foundation Grants MCB-0723931 and ISO-1339239 (to S.L.) and National Natural Science Foundation of China Grants 31270303 (to F.-G.Z.) and 31271626 (to W.L.).

1. Hamburger D, Rezzonico E, MacDonald-Comber Petétot J, Somerville C, Poirier Y (2002) Identification and characterization of the *Arabidopsis PHO1* gene involved in phosphate loading to the xylem. *Plant Cell* 14(4):889–902.
2. Shen J, et al. (2011) Phosphorus dynamics: From soil to plant. *Plant Physiol* 156(3): 997–1005.
3. Shin H, Shin HS, Dewbre GR, Harrison MJ (2004) Phosphate transport in *Arabidopsis*: Pht1;1 and Pht1;4 play a major role in phosphate acquisition from both low- and high-phosphate environments. *Plant J* 39(4):629–642.
4. Ai P, et al. (2009) Two rice phosphate transporters, OsPht1;2 and OsPht1;6, have different functions and kinetic properties in uptake and translocation. *Plant J* 57(5): 798–809.
5. Shane MW, McCully ME, Lambers H (2004) Tissue and cellular phosphorus storage during development of phosphorus toxicity in *Hakea prostrata* (Proteaceae). *J Exp Bot* 55(399):1033–1044.
6. Mimura T, et al. (1990) Phosphate transport across biomembranes and cytosolic phosphate homeostasis in barley leaves. *Planta* 180(2):139–146.
7. Lauer MJ, Blevins DG, Sierzputowska-Gracz H (1989) ^{31}P-nuclear magnetic resonance determination of phosphate compartmentation in leaves of reproductive soybeans (*Glycine max* L.) as affected by phosphate nutrition. *Plant Physiol* 89(4):1331–1336.
8. Pratt J, et al. (2009) Phosphate (Pi) starvation effect on the cytosolic Pi concentration and Pi exchanges across the tonoplast in plant cells: An in vivo ^{31}P-nuclear magnetic resonance study using methylphosphonate as a Pi analog. *Plant Physiol* 151(3): 1646–1657.
9. Secco D, Wang C, Shou H, Whelan J (2012) Phosphate homeostasis in the yeast *Saccharomyces cerevisiae*, the key role of the SPX domain-containing proteins. *FEBS Lett* 586(4):289–295.
10. Hürlimann HC, Stadler-Waibel M, Werner TP, Freimoser FM (2007) Pho91 is a vacuolar phosphate transporter that regulates phosphate and polyphosphate metabolism in *Saccharomyces cerevisiae*. *Mol Biol Cell* 18(11):4438–4445.
11. Secco D, et al. (2012) The emerging importance of the SPX domain-containing proteins in phosphate homeostasis. *New Phytol* 193(4):842–851.
12. Puga MI, et al. (2014) SPX1 is a phosphate-dependent inhibitor of PHOSPHATE STARVATION RESPONSE 1 in *Arabidopsis*. *Proc Natl Acad Sci USA* 111(41):14947–14952.
13. Park BS, Seo JS, Chua NH (2014) NITROGEN LIMITATION ADAPTATION recruits PHOSPHATE2 to target the phosphate transporter PT2 for degradation during the regulation of *Arabidopsis* phosphate homeostasis. *Plant Cell* 26(1):454–464.
14. Lin WY, Huang TK, Chiou TJ (2013) Nitrogen limitation adaptation, a target of microRNA827, mediates degradation of plasma membrane-localized phosphate transporters to maintain phosphate homeostasis in *Arabidopsis*. *Plant Cell* 25(10):4061–4074.
15. Stefanovic A, et al. (2007) Members of the *PHO1* gene family show limited functional redundancy in phosphate transfer to the shoot, and are regulated by phosphate deficiency via distinct pathways. *Plant J* 50(6):982–994.
16. Arpat AB, et al. (2012) Functional expression of PHO1 to the Golgi and *trans*-Golgi network and its role in export of inorganic phosphate. *Plant J* 71(3):479–491.
17. Endler A, et al. (2006) Identification of a vacuolar sucrose transporter in barley and *Arabidopsis* mesophyll cells by a tonoplast proteomic approach. *Plant Physiol* 141(1): 196–207.
18. Wang C, et al. (2012) Functional characterization of the rice SPX-MFS family reveals a key role of OsSPX-MFS1 in controlling phosphate homeostasis in leaves. *New Phytol* 196(1):139–148.
19. Jiang C, Gao X, Liao L, Harberd NP, Fu X (2007) Phosphate starvation root architecture and anthocyanin accumulation responses are modulated by the gibberellin-DELLA signaling pathway in *Arabidopsis*. *Plant Physiol* 145(4):1460–1470.
20. Sakano K, Yazaki Y, Okihara K, Mimura T, Kiyota S (1995) Lack of control in inorganic phosphate uptake by *Catharanthus roseus* (L.) G. Don cells: Cytoplasmic inorganic phosphate homeostasis depends on the tonoplast inorganic phosphate transport system? *Plant Physiol* 108(1):295–302.
21. Hunter PR, Craddock CP, Di Benedetto S, Roberts LM, Frigerio L (2007) Fluorescent reporter proteins for the tonoplast and the vacuolar lumen identify a single vacuolar compartment in *Arabidopsis* cells. *Plant Physiol* 145(4):1371–1382.
22. Hafke JB, Hafke Y, Smith JAC, Lüttge U, Thiel G (2003) Vacuolar malate uptake is mediated by an anion-selective inward rectifier. *Plant J* 35(1):116–128.
23. Raghothama KG (1999) Phosphate acquisition. *Annu Rev Plant Physiol Plant Mol Biol* 50(1):666–693.
24. Fontenot EB, et al. (2015) Increased phosphate transport of *Arabidopsis thaliana* Pht1;1 by site-directed mutagenesis of tyrosine 312 may be attributed to the disruption of homomeric interactions. *Plant Cell Environ* 38(10):2012–2022.
25. Zhang F, et al. (2015) Involvement of OsPht1;4 in phosphate acquisition and mobilization facilitates embryo development in rice. *Plant J* 82(4):556–569.
26. Rausch C, Zimmermann P, Amrhein N, Bucher M (2004) Expression analysis suggests novel roles for the plastidic phosphate transporter Pht2;1 in auto- and heterotrophic tissues in potato and *Arabidopsis*. *Plant J* 39(1):13–28.
27. Guo B, et al. (2008) Functional analysis of the *Arabidopsis* PHT4 family of intracellular phosphate transporters. *New Phytol* 177(4):889–898.
28. Versaw WK, Harrison MJ (2002) A chloroplast phosphate transporter, PHT2;1, influences allocation of phosphate within the plant and phosphate-starvation responses. *Plant Cell* 14(8):1751–1766.
29. Dunlop J, Phung T (1998) Phosphate and slow vacuolar channels in *Beta vulgaris*. *Funct Plant Biol* 25(6):709–718.
30. Ward JM (1997) Patch-clamping and other molecular approaches for the study of plasma membrane transporters demystified. *Plant Physiol* 114(4):1151–1159.
31. De Angeli A, Zhang J, Meyer S, Martinoia E (2013) AtALMT9 is a malate-activated vacuolar chloride channel required for stomatal opening in *Arabidopsis*. *Nat Commun* 4:1804.
32. Pei Z-M, Ward JM, Harper JF, Schroeder JI (1996) A novel chloride channel in *Vicia faba* guard cell vacuoles activated by the serine/threonine kinase, CDPK. *EMBO J* 15(23):6564–6574.
33. Tocquin P, et al. (2003) A novel high-efficiency, low-maintenance, hydroponic system for synchronous growth and flowering of *Arabidopsis thaliana*. *BMC Plant Biol* 3(1):2.
34. Tian QY, Sun P, Zhang WH (2009) Ethylene is involved in nitrate-dependent root growth and branching in *Arabidopsis thaliana*. *New Phytol* 184(4):918–931.
35. John MK (1970) Colorimetric determination of phosphorus in soil and plant materials with ascorbic acid. *Soil Sci* 109(4):214–220.
36. Teng S, Keurentjes J, Bentsink L, Koornneef M, Smeekens S (2005) Sucrose-specific induction of anthocyanin biosynthesis in *Arabidopsis* requires the *MYB75/PAP1* gene. *Plant Physiol* 139(4):1840–1852.
37. Yang K-Y, Liu Y, Zhang S (2001) Activation of a mitogen-activated protein kinase pathway is involved in disease resistance in tobacco. *Proc Natl Acad Sci USA* 98(2): 741–746.
38. Beyhl D, et al. (2009) The *fou2* mutation in the major vacuolar cation channel TPC1 confers tolerance to inhibitory luminal calcium. *Plant J* 58(5):715–723.
39. Bertl A, et al. (1992) Electrical measurements on endomembranes. *Science* 258(5084): 873–874.